Quantifying the Dynamics of Polystyrene Microplastics UV-Aging Process

Ziyi Liu, Yanjie Zhu, Shangsi Lv, Yuxian Shi, Shuofei Dong, Dong Yan, Xiaoshan Zhu, Rong Peng, Arturo A. Keller, and Yuxiong Huang*

Cite This: *Environ. Sci. Technol. Lett.* 2022, 9, 50−56

Read Online

ACCESS | Metrics & More | Article Recommendations | Supporting Information

ABSTRACT: Massive amounts of plastic waste have been released into ecosystems, generating huge amounts of microplastics (MPs) and nanoplastics (NPs) during the environmental aging process. However, particle size and number dynamics along the aging process have not been quantitatively assessed, which can greatly influence their fate and environmental risk assessment. We applied single particle inductively coupled plasma mass spectroscopy (spICP-MS) to quantitatively analyze the polystyrene (PS) MPs aging process with a wide particle size range (800 nm−5 μm) as well as particle number concentration at an environmentally relevant value (down to 7.1×10^6 particles/L). We investigated the UV-light accelerated aging dynamics of PS MPs and revealed the generation of large amounts of nano/microsize PS MPs fragments.

PS MPs showed a rapid size downtrend along the aging process, shrinking from 5 to 1 μm. At the same time, PS MPs particle number concentration increased 3 times. Furthermore, pristine PS MPs may induce acute toxicity in feeding behavior, growth, and survival, while aged ones caused marked chronic toxicity on the reproduction inhibition of *Daphnia magna*, both at environmentally relevant concentrations. Overall, the research uncovered and quantified MPs particle size and concentration during the aging process, which is essential to assessing ecotoxicological risks of MPs/NPs.
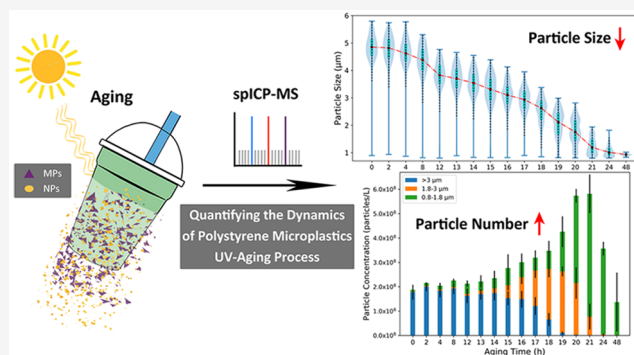
INTRODUCTION

Plastic is a ubiquitous material, and massive amounts of plastics have been released into the environment during their life cycle, with 5000 million metric tons (MMT) of plastic waste accumulated by 2015.[1] During their use and disposal, environmental processes age plastics to generate numerous microplastics (MPs) and nanoplastics (NPs).[2,3] The environmental occurrence and eco-risk of MPs have received more attention globally, as MPs and NPs have been widely detected in environmental media (e.g., aqueous environment, soil, organisms).[4−8] Environmental aging processes generate secondary MPs and NPs, which are the dominant form (∼69%) of MPs and NPs pollution.[9] Studies suggest that environmental aging (e.g., photodegradation and thermo-oxidative degradation) generates and releases about 13 MMT/year of MPs and NPs in water environment,[10] with their size distribution declining.[11,12] However, there are huge knowledge gaps on the quantitative dynamics of aged MPs (NPs are encompassed within the broader MPs category for brevity in this study), which is essential information to assess the associated risks to the ecosystem.[13,14]

The aging process will change the morphology of MPs, which has been extensively studied qualitatively.[15−17] However, accurate quantification of particle numbers and dynamic size changes along the MPs aging process is still lacking. The sizes of MPs along the aging process range from nanoscale (<1 μm) to microscale (<100 μm),[18] which pose huge challenges for conventional MPs analytical techniques to assess particle numbers and size distribution due to the detection limit.[3] For example, micro-Fourier transform infrared spectroscopy (FTIR) can detect MPs down to ∼20 μm,[9] but studies under 5 μm are minimal.[19] Although pyrolysis gas chromatography−mass spectrometry (Py-GC-MS) can analyze MPs at microscale and nanoscale,[20] it is incapable to provide number concentration information. The concentrations of MPs in environmental samples varied in different matrices (∼8×10^3 particles/L in the surface water,[4,21] ∼10^6 particles/L in untreated tap water,[7] and ∼10^5−10^{11} particles/L in wastewater[22]), which makes it arduous and time consuming to analyze MPs by manual counting via imaging methods (e.g., scanning and transmission electron microscopy).[9,23−25]
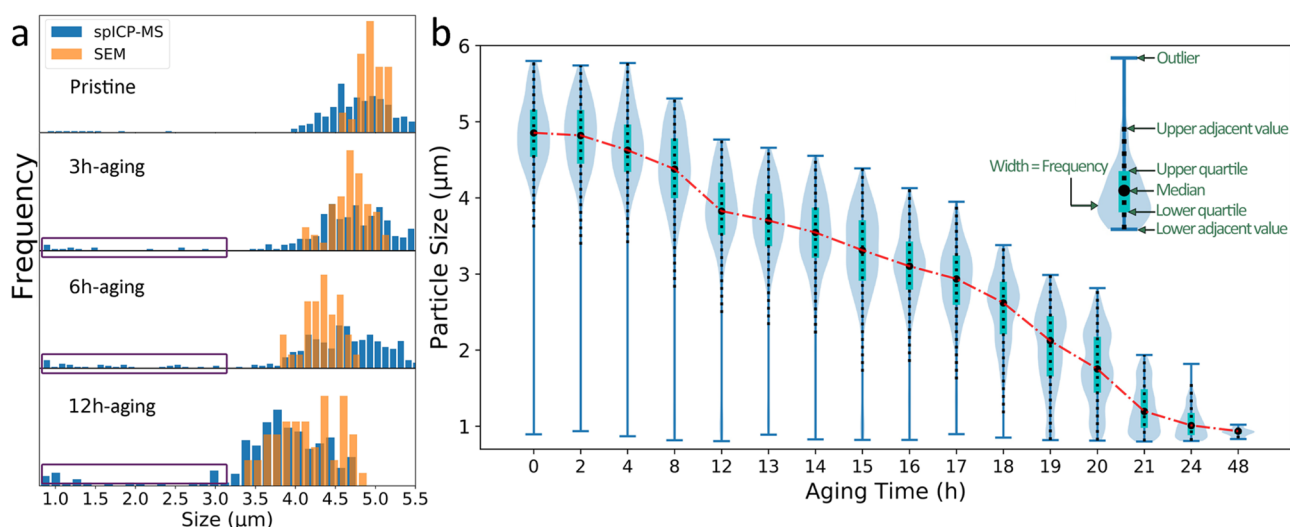
Figure 1. PS MPs particle size distribution determined by (a) spICP-MS and SEM at specific time intervals and (b) spICP-MS along the aging process. In (a), good overlaps between these two techniques were observed. The purple boxes indicated MPs may be breaking down into much smaller pieces along the aging process, during which secondary MPs with sizes at submicrometer to microscale ($\sim$1 μm) were generated in a relatively fast process (after 6-h UV light aging). In (b), the mathematical meanings of the violin plot and scatter points are shown in the upper right. The violin plot displays the median diameter (black dots) and upper and lower quartiles (cyan rectangles) for the size distribution. The upper or lower quartile is the top 25% of numbers in the data set or the 75th percentile. The dotted line represents the upper and lower adjacent values, and the cap of the solid line represents the outlier values. The body of the violin shows widths, which represent particle size frequencies. A clear downtrend in MPs particle size distribution emerged during the aging process.

spICP-MS is a powerful technique to quantitatively analyze nanoparticle numbers and sizes,[26] which has been widely applied for metal-based nanoparticles in environmental matrices.[27−29] Researchers applied spICP-MS to quantify the size and number concentration of the model Au-coated MPs (at submicrometer scale) with a relatively low detection limit (8.4×10^5 particles/L).[30,31] However, this method was based on indirect analysis of the Au coating, which requires multistep sample pretreatment. Recently, it was reported that spICP-MS exhibited the capability to quantify model MPs particle sizes and number concentrations by monitoring ^{13}C,[32,33] which is a promising approach to investigate the dynamics of MPs along the aging process.

To quantify the dynamics of MPs along the aging process, we applied spICP-MS to quantitatively analyze model MPs particle number and size by monitoring the ^{13}C signal in an accelerated aging process. Furthermore, the dynamics of MPs morphology transformation were investigated to better understand the aging process and mechanisms. The ecotoxicological risk was assessed by exposing *Daphnia magna* (*D. magna*) to pristine and aged MPs. We have provided new insights on MPs particle numbers and size dynamics along the aging process as well as the consequential ecotoxicity risk.

■ MATERIALS AND METHODS

Model PS MPs (5 μm, Figure S1) suspensions (10 mg/L) were prepared, and the MPs aging experiments were carried out with a 36 W UV light (Figures S2 and S3). All the PS MPs reference materials were obtained from Agilent Technologies Inc. (Santa Clara, CA, USA). An Agilent 8900 ICP-MS (Agilent Technologies, USA) instrument was used to analyze MPs number concentrations and size distributions by monitoring ^{13}C along the aging process (Table S1). The ecotoxicological assessment was tested with *D. magna* with multidose experiments (0, $\sim$2 $\times$ 10^8, $\sim$3.3 $\times$ 10^8 particles/L,

respectively). Additional details (Tables S2 and S3) are supplied in the Supporting Information S1.

■ RESULTS AND DISCUSSION

Dynamics of PS MPs Sizes along the Aging Process. In our preliminary environmental aging investigation, PS MPs particle sizes were decreased from >40 μm to $\sim$25 μm (Figure S4) after 2-year aging in surface water, which agreed with the previous report.[34] However, it is a huge challenge to reveal the quantitative dynamics of MPs particle sizes and numbers in a natural aging process with an imaging analysis approach.[35,36] UV light was widely adapted to accelerate the environmental aging process,[37,38] which provides good simulation to environmentally realistic conditions.[39,40] Thus, the aging process of model PS MPs was performed on a UV-light controllable and accelerated system (Figures S2 and S3) with an average irradiance of 75.2 W/m^2 at 254 nm. A 24-h UV aging time was equivalent to about 3−8 years of sunlight aging time in the northern hemisphere, based on conversion of the solar radiation spectrum and UV radiation constitutes.[41−44]

As is illustrated in Supporting Information S2, spICP-MS could provide convenient and accurate quantification of MPs particle sizes and number concentrations (Figures S5 and S6; Tables S4 and S5) with a wide size range (Figure S7) covering submicrometer to microscale (<5 μm), and with low number concentration LOD (Figure S8). Good consistency of quantitative analysis could be achieved in different environmental matrices (Table S6). Scanning electron microscopy (SEM) and spICP-MS were applied to determine MPs particle size distribution, showing good consistency (Figure 1a; Table S7). The MPs sizes gradually decreased from 5 to 4.3 μm after 6 h of aging (Figure 1a), revealing the MPs size reduction in the environmental aging process. Similar downsizing patterns were reported by using a fragmentation model to study the MPs environment aging process.[12] In addition, a wider size distribution was observed after 12 h of aging, suggesting MPs
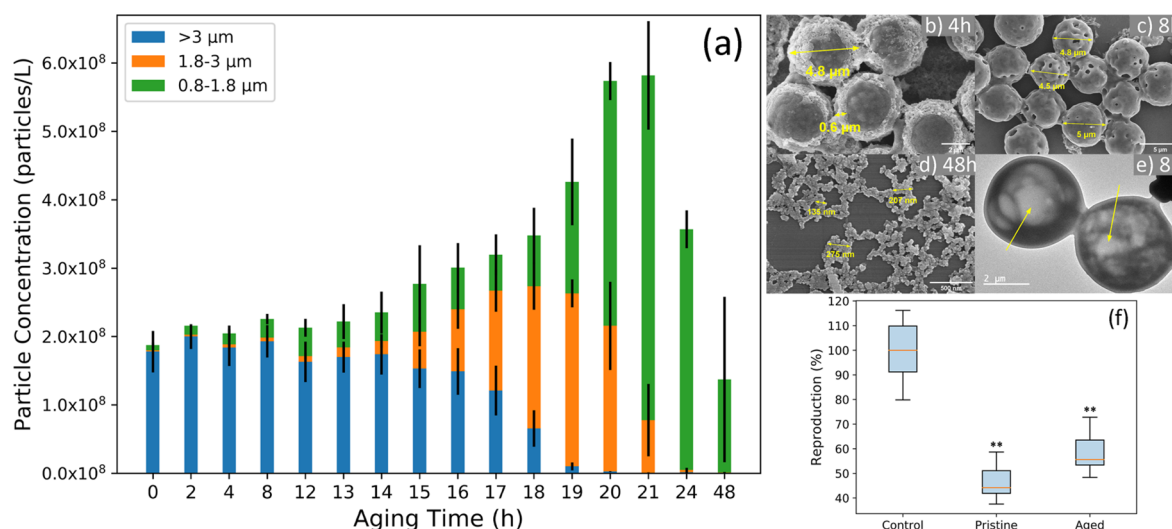
Figure 2. (a) PS MPs particle number concentration along the aging process determined by spICP-MS. (b−e) PS MPs morphological changes along the aging process. (f) Effect of pristine and aged PS MPs on *D. magna*. In (a), both total and size-fractionated particle number concentrations were presented, showing concentration increase and smaller secondary MPs generation. In (b−e), changes in PS MPs morphology were monitored by SEM (b−d) and TEM (e), showing a size decrease and structure breakdown. Double arrows in (b−d) display the size of PS MPs, and single arrows in (e) display hollow structures along the aging dynamics. In (f), reproduction during a 21-day exposure was shown, and the comparison between the control group (100%) and pristine/aged PS MPs group was presented to demonstrate the eco-effect of pristine/aged MPs. Asterisks indicate the statistical significance ($p < 0.05$, ANOVA).

may be breaking down into much smaller pieces during the aging process, as highlighted by the purple boxes in Figure 1a. Prior studies had also noted that MPs would experience elongation and breakdown to smaller pieces during sunlight aging with microscopy observation,[45] which may result in a wider size range.

Although Figure 1a shows good correlations for particles >3 μm, smaller MPs particles may be neglected by SEM imaging as the limited view due to the sample preparation, which may not cover the full range of MPs from submicrometer to microscale (<5 μm). Furthermore, the particle size distribution of MPs as determined by imaging calibration tools (e.g., ImageJ) highly depends on sample numbers and operator subjectivity. As indicated by purple boxes in Figure 1a, spICP-MS detected the generation of small granules along the aging process, which was missed by SEM imaging. On the basis of the spICP-MS measurements (Figure 1a), the aging process generates secondary MPs with sizes at submicrometer to microscale (~1 μm), which was a relatively fast process (after 6-h UV light aging). Thus, we have identified and quantified the secondary MPs generated along the aging process via spICP-MS, which would have been missed in the previous studies.

Given the ease of measuring particle size distribution with spICP-MS, the dynamics of the MPs aging process can be tracked in considerable detail (Figure 1b), providing additional insights. The particle size distribution did not change substantially during the first 4 h of aging (Figure 1b), although the median particle size decreased slightly (from 4.8 to 4.6 μm). The shrinking size may be attributed to the formation of small cavities on the MPs surfaces.[46] Clear changes in MPs particle size distribution emerged after 8 h of aging and subsequently revealed the downward trend in size due to aging. The median size decreased to 4.5 and 3.3 μm after 8 h and 16 h of aging, respectively, and then more rapidly reduced to ~1.3 μm after 24 h (Figure 1b), as the particles began to break down into much smaller pieces.[46,47]

Eventually, the median particle size decreased to ~1 μm with a narrow distribution after 48 h (Figure 1b). However, due to the ^{13}C background signal interference, the size detection limit of spICP-MS is 800 nm. A significant number of submicrometer-scale MPs (<800 nm) generated by the aging process may not be detected in the present study, which is still a challenge for the analysis of NPs. Nonetheless, we have quantitatively investigated the size dynamics of MPs at the low end (down to 800 nm) via spICP-MS, which was a missing piece of the information to understand their aging process.[19]

Dynamics of PS MPs Particle Number Concentration during Aging. In addition to the particle size distribution, the MPs particle number concentration dynamics along the aging process were monitored by spICP-MS (Figure 2a). The total particle number concentration did not exhibit an obvious uptrend during the first 12 h, indicating that there was no significant amount of secondary MPs generation but a slight decrease in particle size (Figure 1). A rapid increase in particle number concentration was observed after 12 h and subsequently, with the total carbon mass remaining stable along the aging process (Figure S9). The total particle number concentration peaked (~6 × 10^8 particles/L) after 20 h, which was 3 times greater than the pristine MPs initial concentration (~2 × 10^8 particles/L). Thus, the aging process induced a noticeable increase in the total number of MPs in the environment.[11]

To further understand the dynamics of MPs particle number concentration during the aging process, size-fractionated (>3 μm, 1.8−3 μm, and 0.8−1.8 μm) particle number concentrations were obtained by spICP-MS (Figure 2a). Similar to the trend of MPs total particle number concentration, MPs size-fractionated particle number concentrations display no significant differences in the first 8-h aging process. After 12 h of aging, the particle number concentration of midsize (1.8−3 μm) MPs has been continually increased and reached a peak (2.5 × 10^8 particles/L) at the 19th hour, while the large-sized (>3 μm) MPs particle number concentration declined to 0. It

suggests that the MPs began to break down into smaller, aged MPs via various processes (e.g., photolysis, erosion, fragmentation).[18,48] Meanwhile, there was a marked growth of the particle number concentration of the smaller MPs (0.8−1.8 μm), from approximately 0.3×10^8 to 1.7×10^8 particles/L (Figure 2a), indicating the generation of smaller secondary MPs along the aging process. After 20 h of aging, the MPs population was dominated by smaller size MPs (0.8−1.8 μm), whose particle number concentration peaked ($\sim 5 \times 10^8$ particles/L) in the 21st hour, while those of both mid-sized and large-sized MPs decreased to 0. In addition, the particle number concentration of the smaller MPs showed a descending tendency after 24 h of aging ($\sim 3.3 \times 10^8$ particles/L), which reflects the analytical limits of the current spICP-MS method in the submicrometer scale (<800 nm). Despite that, our current study has advanced the quantitative analytical limits of MPs to the submicrometer scale ($\sim$800 nm) at environmental relevant concentrations and revealed the "hidden" generation and accumulation of secondary MPs (<3 μm) along the aging process.

PS MPs Morphological Changes during Aging. MPs morphology change during the aging process was monitored by SEM and transmission electron microscopy (TEM) (Figure 2b−e; Figure S10). In the first 4 h, the MPs began to form a core−shell structure (Figure 2b), suggesting that MPs experienced dissolution,[49] followed by the exfoliation of small pieces from the MPs surfaces. In addition, fragments with sizes from 0.17 to 0.53 μm were observed (Figure S10a and f), matching the dimensions of the peeling layer ($\sim$0.6 μm) of the aged MPs (Figure 2b), further confirming that submicrometer-scale MPs would be stripped from the surface of pristine MPs to generate secondary MPs. Notably, cavities (Figure 2c) and hollow structures (Figure 2e) were observed on the MPs surfaces after 8 h, which may be attributed to the embrittlement of the polymer's backbone due to UV oxidation.[50] After 10 h, deformation of the MPs spherical structures and cross-linking was observed (Figure S10b), induced by the UV-light aging process.[51] MPs were completely damaged (Figure S10c−e) and broken into small-size secondary MPs with cavities (Figure S10g) and hollow structures (Figure S10h) after 15 h. Only submicrometer-scale (100−300 nm) MPs with flocculent morphology were observed after 48 h (Figure 2d).

Ecotoxicological Risk of PS MPs. The ecotoxicological risk of MPs during aging was evaluated by exposing *D. magna* to pristine and aged MPs at environmentally relevant concentrations. As filter-feeding plankton, *D. magna* feeding behavior was significantly inhibited after a 24-h exposure to pristine MPs, showing a ~60% reduction in food intake compared to the control group (Figure S11a). Compared with pristine MPs (Figure S12a), we observed the agglomeration of MPs and algae during the exposure (Figure S12b), which may reduce algae bioavailability and feeding efficiency of *D. magna*. Furthermore, the agglomerated MPs and algae adhered to the thoracic limbs of *D. magna* (Figure S13), which may inhibit *D. magna* swimming behavior and feeding efficiency. The decrease in feeding efficiency led to a significant decrease in *D. magna* body length (Figure S11b), which further resulted in notable lower survival (~30%) compared to the control (Figure S11c) after a 7-day exposure to pristine MPs. Notably, a significant amount of MPs was found in the intestinal tract of *D. magna* (Figure S12c), which was also found in other organisms[52] and disrupted the *D. magna* digestion system,

hindering their survival and growth.[53,54] Additionally, *D. magna* offspring were significantly delayed in the 21-day exposure (Figure S14), with a ~60% decrease in reproduction compared to the control (Figure 2f), which is likely due to the lower feeding and energetic deficiencies.[55] Thus, being exposed to pristine MPs would significantly inhibit *D. magna* feeding behavior, growth, survival, and reproduction due to the changes in swimming behavior, feeding behavior constraints, and digestion system disruption.

As discussed above, after 24 h of aging, the median size of the MPs decreased from 5 to $\sim$1 μm, while the particle number concentration increased 3-fold, which would change the ecotoxicological risks to *D. magna*. Surprisingly, compared to the control, there were no significant differences in *D. magna* feeding efficiency, body length, and survival after exposure to aged MPs (Figure S11). The smaller size of the aged MPs ($\sim$1 μm) may not induce adverse effects on *D. magna* as few MPs were observed in the intestines of *D. magna* in the optical microscope (Figure S12d), which may result from the *D. magna* depuration and egestion process[56,57] and further reduce acute toxicity.[58] On the other hand, the *D. magna* first brood time exhibited a significant delay after exposure to aged MPs (Figure S14) with a notable drop in the quantity of offspring (~40%) compared to the control (Figure 2f). The amplified multigenerational effect of both the pristine and aged MPs may be due to the exhaustion of maternal energy during exposure[59] and induced sublethal effects to the subsequent generation.[58] Thus, with the sustainable increase in particle number and unknown leachates, the aged MPs may induce marked chronic toxicity (e.g., inhibit reproduction) during long-term exposure, which requires more investigation in the future.

Environmental Implications. We quantitatively revealed the dynamics of MPs particle size (0.8−5 μm) and number along the accelerated aging process with the spICP-MS method, based on the indicated environmental aging trend. The study demonstrated that submicrometer-scale secondary MPs (<3 μm) were generated at a relatively fast rate (up to $\sim$67% annual increase of the particle number) along the environmental aging process, which was overlooked in previous studies and acts as a "hidden" threat to ecosystems.[60] With vast global plastic wastes produced and ~79% of them accumulated in the environment,[61,62] the generation of secondary MPs due to the environmental aging process (estimated 13 MMT per year)[10] should be considered as a critical source of MPs in the environment,[14] while having not been previously quantified. Therefore, our research uncovered the quantification dynamics of particle sizes and number concentrations of MPs along the aging process, which provides essential information to properly estimate and predict the long-term fate as well as the retention of MPs in the environment. Furthermore, the aged MPs may induce chronic toxicity (e.g., inhibited reproduction) during long-term exposure, posing "hidden" ecotoxicological risks and demanding more attention and investigation due to their pervasive distribution in the environment.[63−65] Overall inclusively, we have investigated the MPs environmental aging process, filling the knowledge gap on the quantitative dynamics of MPs particle sizes and number concentrations, which present new approaches on the analysis of the MPs fate and ecotoxicological risks.

ASSOCIATED CONTENT

S1 Supporting Information

The Supporting Information is available free of charge at https://pubs.acs.org/doi/10.1021/acs.estlett.1c00888.

Materials and methods details (S1), quantitative analysis of PS MPs by spICP-MS (S2), SEM images of PS MPs (Figure S1), UV-light experiment setup (Figure S2), spectral distribution of the 254 nm UV lamp (Figure S3), SEM images and size distribution of pristine and aged raw PS MPs (Figure S4), PS MPs particle size distribution determined by spICP-MS and SEM (Figure S5), PS MPs particle size distribution determined by spICP-MS (Figure S6), calibration curve of PS MPs size and number concentration by spICP-MS (Figure S7 and S8), total organic carbon change during PS MPs aging process (Figure S9), PS MPs morphological changes along the aging process (Figure S10), effect of pristine and aged PS MPs on *D. magna* (Figure S11), optical microscope images of *D. magna* exposed in pristine and aged PS MPs (Figures S12 and S13), reproduction trend of *D. magna* (Figure S14), spICP-MS instrumental details (Table S1), composition of MHRW (Table S2), parameters for nebulization efficiency calculation (Table S3), size specification of commercial PS MPs (Table S4), number concentrations consistency of iron-doped PS MPs (Table S5), quantitative analytical consistency in DIW and seawater determined by spICP-MS (Table S6), determined size by spICP-MS and SEM during the aging process (Table S7), nebulization efficiency formula (eq S1), size calibration curve (eq S2), and number concentration LOD (eq S3) (PDF)

AUTHOR INFORMATION

Corresponding Author

Yuxiong Huang — *Tsinghua-Berkeley Shenzhen Institute (TBSI), Tsinghua Shenzhen International Graduate School (SIGS), Tsinghua University, Shenzhen 518055, China;* orcid.org/0000-0001-8124-643X; Phone: +86 0755 2640 3079; Email: huang_yuxiong@sz.tsinghua.edu.cn

Authors

Ziyi Liu — *Tsinghua-Berkeley Shenzhen Institute (TBSI), Tsinghua Shenzhen International Graduate School (SIGS), Tsinghua University, Shenzhen 518055, China*

Yanjie Zhu — *Tsinghua-Berkeley Shenzhen Institute (TBSI), Tsinghua Shenzhen International Graduate School (SIGS), Tsinghua University, Shenzhen 518055, China*

Shangsi Lv — *Tsinghua-Berkeley Shenzhen Institute (TBSI), Tsinghua Shenzhen International Graduate School (SIGS), Tsinghua University, Shenzhen 518055, China*

Yuxian Shi — *Tsinghua-Berkeley Shenzhen Institute (TBSI), Tsinghua Shenzhen International Graduate School (SIGS), Tsinghua University, Shenzhen 518055, China*

Shuofei Dong — *Agilent Technologies Co., Ltd., Beijing 100102, China*

Dong Yan — *Agilent Technologies Co., Ltd., Beijing 100102, China*

Xiaoshan Zhu — *Tsinghua-Berkeley Shenzhen Institute (TBSI), Tsinghua Shenzhen International Graduate School (SIGS), Tsinghua University, Shenzhen 518055, China;* orcid.org/0000-0003-1223-1415

Rong Peng — *Tsinghua-Berkeley Shenzhen Institute (TBSI), Tsinghua Shenzhen International Graduate School (SIGS), Tsinghua University, Shenzhen 518055, China*

Arturo A. Keller — *Bren School of Environmental Science and Management, University of California, Santa Barbara, California 93106, United States;* orcid.org/0000-0002-7638-662X

Complete contact information is available at:
https://pubs.acs.org/10.1021/acs.estlett.1c00888

Notes

The authors declare no competing financial interest.

ACKNOWLEDGMENTS

REFERENCES

(1) Geyer, R.; Jambeck, J. R.; Law, K. L. Production, Use, and Fate of All Plastics Ever Made. *Sci. Adv.* **2017**, *3* (7), No. e1700782.

(2) Ding, L.; Mao, R.; Ma, S.; Guo, X.; Zhu, L. High Temperature Depended on the Ageing Mechanism of Microplastics under Different Environmental Conditions and Its Effect on the Distribution of Organic Pollutants. *Water Res.* **2020**, *174*, 115634.

(3) Alimi, O. S.; Farner Budarz, J.; Hernandez, L. M.; Tufenkji, N. Microplastics and Nanoplastics in Aquatic Environments: Aggregation, Deposition, and Enhanced Contaminant Transport. *Environ. Sci. Technol.* **2018**, *52* (4), 1704−1724.

(4) Li, Y.; Li, W.; Jarvis, P.; Zhou, W.; Zhang, J.; Chen, J.; Tan, Q.; Tian, Y. Occurrence, Removal and Potential Threats Associated with Microplastics in Drinking Water Sources. *J. Environ. Chem. Eng.* **2020**, *8* (6), 104527.

(5) Sikder, M.; Wang, J.; Poulin, B. A.; Tfaily, M. M.; Baalousha, M. Nanoparticle Size and Natural Organic Matter Composition Determine Aggregation Behavior of Polyvinylpyrrolidone Coated Platinum Nanoparticles. *Environ. Sci.: Nano* **2020**, *7*, 3318.

(6) Skaf, D. W.; Punzi, V. L.; Rolle, J. T.; Kleinberg, K. A. Removal of Micron-Sized Microplastic Particles from Simulated Drinking Water via Alum Coagulation. *Chem. Eng. J.* **2020**, *386*, 123807.

(7) Koelmans, A. A.; Mohamed Nor, N. H.; Hermsen, E.; Kooi, M.; Mintenig, S. M.; De France, J. Microplastics in Freshwaters and Drinking Water: Critical Review and Assessment of Data Quality. *Water Res.* **2019**, *155*, 410−422.

(8) de Sá, L. C.; Oliveira, M.; Ribeiro, F.; Rocha, T. L.; Futter, M. N. Studies of the Effects of Microplastics on Aquatic Organisms: What Do We Know and Where Should We Focus Our Efforts in the Future? *Sci. Total Environ.* **2018**, *645*, 1029−1039.

(9) Li, J.; Liu, H.; Paul Chen, J. Microplastics in Freshwater Systems: A Review on Occurrence, Environmental Effects, and Methods for Microplastics Detection. *Water Res.* **2018**, *137*, 362−374.

(10) Dees, J. P.; Ateia, M.; Sanchez, D. L. Microplastics and Their Degradation Products in Surface Waters: A Missing Piece of the Global Carbon Cycle Puzzle. *ACS EST Water* **2021**, *1* (2), 214−216.

(11) Rillig, M. C.; Kim, S. W.; Kim, T.-Y.; Waldman, W. R. The Global Plastic Toxity Debt. *Environ. Sci. Technol.* **2021**, *55*, 2717.

(12) Wang, L.; Li, P.; Zhang, Q.; Wu, W.-M.; Luo, J.; Hou, D. Modeling the Conditional Fragmentation-Induced Microplastic Distribution. *Environ. Sci. Technol.* **2021**, *55*, 6012.

(13) Wei, X.-F.; Nilsson, F.; Yin, H.; Hedenqvist, M. S. Microplastics Originating from Polymer Blends: An Emerging Threat? *Environ. Sci. Technol.* **2021**, *55*, 4190.

(14) de Ruijter, V. N.; Redondo-Hasselerharm, P. E.; Gouin, T.; Koelmans, A. A. Quality Criteria for Microplastic Effect Studies in the Context of Risk Assessment: A Critical Review. *Environ. Sci. Technol.* **2020**, *54* (19), 11692−11705.

(15) Chamas, A.; Moon, H.; Zheng, J.; Qiu, Y.; Tabassum, T.; Jang, J. H.; Abu-Omar, M.; Scott, S. L.; Suh, S. Degradation Rates of Plastics in the Environment. *ACS Sustainable Chem. Eng.* **2020**, *8* (9), 3494−3511.

(16) Wang, X.; Li, Y.; Zhao, J.; Xia, X.; Shi, X.; Duan, J.; Zhang, W. UV-Induced Aggregation of Polystyrene Nanoplastics: Effects of Radicals, Surface Functional Groups and Electrolyte. *Environ. Sci.: Nano* **2020**, *7*, 3914.

(17) ter Halle, A.; Ladirat, L.; Martignac, M.; Mingotaud, A. F.; Boyron, O.; Perez, E. To What Extent Are Microplastics from the Open Ocean Weathered? *Environ. Pollut.* **2017**, *227*, 167−174.

(18) Horton, A. A.; Walton, A.; Spurgeon, D. J.; Lahive, E.; Svendsen, C. Microplastics in Freshwater and Terrestrial Environments: Evaluating the Current Understanding to Identify the Knowledge Gaps and Future Research Priorities. *Sci. Total Environ.* **2017**, *586*, 127−141.

(19) Oßmann, B. E.; Sarau, G.; Holtmannspötter, H.; Pischetsrieder, M.; Christiansen, S. H.; Dicke, W. Small-Sized Microplastics and Pigmented Particles in Bottled Mineral Water. *Water Res.* **2018**, *141*, 307−316.

(20) Ter Halle, A.; Jeanneau, L.; Martignac, M.; Jardé, E.; Pedrono, B.; Brach, L.; Gigault, J. Nanoplastic in the North Atlantic Subtropical Gyre. *Environ. Sci. Technol.* **2017**, *51* (23), 13689−13697.

(21) Wang, Z.; Lin, T.; Chen, W. Occurrence and Removal of Microplastics in an Advanced Drinking Water Treatment Plant (ADWTP). *Sci. Total Environ.* **2020**, *700*, 134520.

(22) Enfrin, M.; Lee, J.; Gibert, Y.; Basheer, F.; Kong, L.; Dumée, L. F. Release of Hazardous Nanoplastic Contaminants Due to Microplastics Fragmentation under Shear Stress Forces. *J. Hazard. Mater.* **2020**, *384*, 121393.

(23) Ni, B.-J.; Zhu, Z.-R.; Li, W.-H.; Yan, X.; Wei, W.; Xu, Q.; Xia, Z.; Dai, X.; Sun, J. Microplastics Mitigation in Sewage Sludge through Pyrolysis: The Role of Pyrolysis Temperature. *Environ. Sci. Technol. Lett.* **2020**, *7* (12), 961−967.

(24) Wang, W.; Wang, J. Investigation of Microplastics in Aquatic Environments: An Overview of the Methods Used, from Field Sampling to Laboratory Analysis. *TrAC, Trends Anal. Chem.* **2018**, *108*, 195−202.

(25) Dalla Fontana, G.; Mossotti, R.; Montarsolo, A. Assessment of Microplastics Release from Polyester Fabrics: The Impact of Different Washing Conditions. *Environ. Pollut.* **2020**, *264*, 113960.

(26) Laborda, F.; Gimenez-Ingalaturre, A. C.; Bolea, E.; Castillo, J. R. Single Particle Inductively Coupled Plasma Mass Spectrometry as Screening Tool for Detection of Particles. *Spectrochim. Acta, Part B* **2019**, *159*, 105654.

(27) Keller, A. A.; Huang, Y.; Nelson, J. Detection of Nanoparticles in Edible Plant Tissues Exposed to Nano-Copper Using Single-Particle ICP-MS. *J. Nanopart. Res.* **2018**, *20* (4), 101.

(28) Huang, Y.; Keller, A. A.; Cervantes-Avilés, P.; Nelson, J. Fast Multielement Quantification of Nanoparticles in Wastewater and Sludge Using Single-Particle ICP-MS. *ACS EST Water* **2021**, *1*, 205.

(29) Cervantes-Avilés, P.; Huang, Y.; Keller, A. A. Incidence and Persistence of Silver Nanoparticles throughout the Wastewater Treatment Process. *Water Res.* **2019**, *156*, 188−198.

(30) Lai, Y.; Dong, L.; Li, Q.; Li, P.; Hao, Z.; Yu, S.; Liu, J. Counting Nanoplastics in Environmental Waters by Single Particle Inductively Coupled Plasma Mass Spectroscopy after Cloud-Point Extraction and *In Situ* Labeling of Gold Nanoparticles. *Environ. Sci. Technol.* **2021**, *55*, 4783.

(31) Jiménez-Lamana, J.; Marigliano, L.; Allouche, J.; Grassl, B.; Szpunar, J.; Reynaud, S. A Novel Strategy for the Detection and Quantification of Nanoplastics by Single Particle Inductively Coupled Plasma Mass Spectrometry (ICP-MS). *Anal. Chem.* **2020**, *92* (17), 11664−11672.

(32) Bolea-Fernandez, E.; Rua-Ibarz, A.; Velimirovic, M.; Tirez, K.; Vanhaecke, F. Detection of Microplastics Using Inductively Coupled Plasma-Mass Spectrometry (ICP-MS) Operated in Single-Event Mode. *J. Anal. At. Spectrom.* **2020**, *35* (3), 455−460.

(33) Laborda, F.; Trujillo, C.; Lobinski, R. Analysis of Microplastics in Consumer Products by Single Particle-Inductively Coupled Plasma Mass Spectrometry Using the Carbon-13 Isotope. *Talanta* **2021**, *221*, 121486.

(34) El Hadri, H.; Gigault, J.; Maxit, B.; Grassl, B.; Reynaud, S. Nanoplastic from Mechanically Degraded Primary and Secondary Microplastics for Environmental Assessments. *NanoImpact* **2020**, *17*, 100206.

(35) Blancho, F.; Davranche, M.; Hadri, H. E.; Grassl, B.; Gigault, J. Nanoplastics Identification in Complex Environmental Matrices: Strategies for Polystyrene and Polypropylene. *Environ. Sci. Technol.* **2021**, *55*, 8753.

(36) Li, C.; Gao, Y.; He, S.; Chi, H.-Y.; Li, Z.-C.; Zhou, X.-X.; Yan, B. Quantification of Nanoplastic Uptake in Cucumber Plants by Pyrolysis Gas Chromatography/Mass Spectrometry. *Environ. Sci. Technol. Lett.* **2021**, *8*, 633.

(37) Meides, N.; Menzel, T.; Poetzschner, B.; Löder, M. G. J.; Mansfeld, U.; Strohriegl, P.; Altstaedt, V.; Senker, J. Reconstructing the Environmental Degradation of Polystyrene by Accelerated Weathering. *Environ. Sci. Technol.* **2021**, *55* (12), 7930−7938.

(38) Wu, X.; Liu, P.; Wang, H.; Huang, H.; Shi, Y.; Yang, C.; Gao, S. Photo Aging of Polypropylene Microplastics in Estuary Water and Coastal Seawater: Important Role of Chlorine Ion. *Water Res.* **2021**, *202*, 117396.

(39) Fan, X.; Zou, Y.; Geng, N.; Liu, J.; Hou, J.; Li, D.; Yang, C.; Li, Y. Investigation on the Adsorption and Desorption Behaviors of Antibiotics by Degradable MPs with or without UV Ageing Process. *J. Hazard. Mater.* **2021**, *401*, 123363.

(40) Wang, Z.; An, C.; Chen, X.; Lee, K.; Zhang, B.; Feng, Q. Disposable Masks Release Microplastics to the Aqueous Environment with Exacerbation by Natural Weathering. *J. Hazard. Mater.* **2021**, *417*, 126036.

(41) Sengupta, M.; Xie, Y.; Lopez, A.; Habte, A.; Maclaurin, G.; Shelby, J. The National Solar Radiation Data Base (NSRDB). *Renewable Sustainable Energy Rev.* **2018**, *89*, 51−60.

(42) Gueymard, C. A. Solar Radiation Spectrum. In *Encyclopedia of Sustainability Science and Technology*; Meyers, R. A., Ed.; Springer: New York, 2013; pp 1−32. DOI: 10.1007/978-1-4939-2493-6_445-3.

(43) Coddington, O.; Lean, J. L.; Lindholm, D.; Pilewskie, P.; Snow, M. *NOAA Climate Data Record (CDR) of Solar Spectral Irradiance (SSI)*, NRLSSI Version 2; NOAA CDR Program, 2015. DOI: 10.7289/V51J97P6.

(44) Andrade, J.; Fernández-González, V.; López-Mahía, P.; Muniategui, S. A Low-Cost System to Simulate Environmental Microplastic Weathering. *Mar. Pollut. Bull.* **2019**, *149*, 110663.

(45) Brandon, J.; Goldstein, M.; Ohman, M. D. Long-Term Aging and Degradation of Microplastic Particles: Comparing in Situ Oceanic and Experimental Weathering Patterns. *Mar. Pollut. Bull.* **2016**, *110* (1), 299−308.

(46) Mao, R.; Lang, M.; Yu, X.; Wu, R.; Yang, X.; Guo, X. Aging Mechanism of Microplastics with UV Irradiation and Its Effects on the Adsorption of Heavy Metals. *J. Hazard. Mater.* **2020**, *393*, 122515.

(47) Lambert, S.; Wagner, M. Characterisation of Nanoplastics during the Degradation of Polystyrene. *Chemosphere* **2016**, *145*, 265−268.

(48) da Costa, J. P.; Santos, P. S. M.; Duarte, A. C.; Rocha-Santos, T. (Nano)Plastics in the Environment − Sources, Fates and Effects. *Sci. Total Environ.* **2016**, *566−567*, 15−26.

(49) Tian, L.; Chen, Q.; Jiang, W.; Wang, L.; Xie, H.; Kalogerakis, N.; Ma, Y.; Ji, R. A Carbon-14 Radiotracer-Based Study on the Phototransformation of Polystyrene Nanoplastics in Water versus in Air. *Environ. Sci.: Nano* **2019**, *6* (9), 2907−2917.

(50) Cundiff, K. N.; Madi, Y.; Benzerga, A. A. Photo-Oxidation of Semicrystalline Polymers: Damage Nucleation versus Growth. *Polymer* **2020**, *188*, 122090.

(51) Rodriguez, A. K.; Mansoor, B.; Ayoub, G.; Colin, X.; Benzerga, A. A. Effect of UV-Aging on the Mechanical and Fracture Behavior of Low Density Polyethylene. *Polym. Degrad. Stab.* **2020**, *180*, 109185.

(52) Liu, X.; Wang, J. Algae (Raphidocelis Subcapitata) Mitigate Combined Toxicity of Microplastic and Lead on Ceriodaphnia Dubia. *Front. Environ. Sci. Eng.* **2020**, *14* (6), 97.

(53) Lovern, S. B.; Strickler, J. R.; Klaper, R. Behavioral and Physiological Changes in Daphnia Magna When Exposed to Nanoparticle Suspensions (Titanium Dioxide, Nano-C60, and C60HxC70Hx). *Environ. Sci. Technol.* **2007**, *41* (12), 4465−4470.

(54) Pikuda, O.; Xu, E. G.; Berk, D.; Tufenkji, N. Toxicity Assessments of Micro- and Nanoplastics Can Be Confounded by Preservatives in Commercial Formulations. *Environ. Sci. Technol. Lett.* **2019**, *6* (1), 21−25.

(55) Yu, J.; Tian, J.-Y.; Xu, R.; Zhang, Z.-Y.; Yang, G.-P.; Wang, X.-D.; Lai, J.-G.; Chen, R. Effects of Microplastics Exposure on Ingestion, Fecundity, Development, and Dimethylsulfide Production in Tigriopus Japonicus (Harpacticoida, Copepod). *Environ. Pollut.* **2020**, *267*, 115429.

(56) Elizalde-Velázquez, A.; Carcano, A. M.; Crago, J.; Green, M. J.; Shah, S. A.; Cañas-Carrell, J. E. Translocation, Trophic Transfer, Accumulation and Depuration of Polystyrene Microplastics in Daphnia Magna and Pimephales Promelas. *Environ. Pollut.* **2020**, *259*, 113937.

(57) Wang, Y.; Mao, Z.; Zhang, M.; Ding, G.; Sun, J.; Du, M.; Liu, Q.; Cong, Y.; Jin, F.; Zhang, W.; Wang, J. The Uptake and Elimination of Polystyrene Microplastics by the Brine Shrimp, Artemia Parthenogenetica, and Its Impact on Its Feeding Behavior and Intestinal Histology. *Chemosphere* **2019**, *234*, 123−131.

(58) Xu, E. G.; Cheong, R. S.; Liu, L.; Hernandez, L. M.; Azimzada, A.; Bayen, S.; Tufenkji, N. Primary and Secondary Plastic Particles Exhibit Limited Acute Toxicity but Chronic Effects on *Daphnia Magna*. *Environ. Sci. Technol.* **2020**, *54* (11), 6859−6868.

(59) Schür, C.; Zipp, S.; Thalau, T.; Wagner, M. Microplastics but Not Natural Particles Induce Multigenerational Effects in Daphnia Magna. *Environ. Pollut.* **2020**, *260*, 113904.

(60) Mitrano, D. M.; Wick, P.; Nowack, B. Placing Nanoplastics in the Context of Global Plastic Pollution. *Nat. Nanotechnol.* **2021**, *16*, 491.
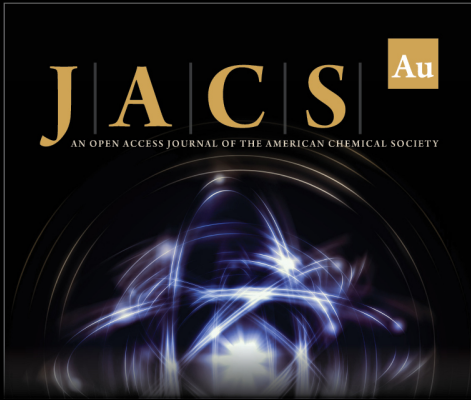
(61) Stubbins, A.; Law, K. L.; Muñoz, S. E.; Bianchi, T. S.; Zhu, L. Plastics in the Earth System. *Science* **2021**, *373* (6550), 51−55.

(62) MacLeod, M.; Arp, H. P. H.; Tekman, M. B.; Jahnke, A. The Global Threat from Plastic Pollution. *Science* **2021**, *373* (6550), 61−65.

(63) Ross, P. S.; Chastain, S.; Vassilenko, E.; Etemadifar, A.; Zimmermann, S.; Quesnel, S.-A.; Eert, J.; Solomon, E.; Patankar, S.; Posacka, A. M.; Williams, B. Pervasive Distribution of Polyester Fibres in the Arctic Ocean Is Driven by Atlantic Inputs. *Nat. Commun.* **2021**, *12* (1), 106.

(64) Santos, R. G.; Machovsky-Capuska, G. E.; Andrades, R. Plastic Ingestion as an Evolutionary Trap: Toward a Holistic Understanding. *Science* **2021**, *373* (6550), 56−60.

(65) Du, M.; Peng, X.; Zhang, H.; Ye, C.; Dasgupta, S.; Li, J.; Li, J.; Liu, S.; Xu, H.; Chen, C.; Jing, H.; Xu, H.; Liu, J.; He, S.; He, L.; Cai, S.; Chen, S.; Ta, K. Geology, Environment, and Life in the Deepest Part of the World's Oceans. *Innovation* **2021**, *2* (2), 100109.